

# We are IntechOpen, the world's leading publisher of Open Access books Built by scientists, for scientists

**4,800**

Open access books available

**122,000**

International authors and editors

**135M**

Downloads

Our authors are among the

**154**

Countries delivered to

**TOP 1%**

most cited scientists

**12.2%**

Contributors from top 500 universities



**WEB OF SCIENCE™**

Selection of our books indexed in the Book Citation Index  
in Web of Science™ Core Collection (BKCI)

Interested in publishing with us?  
Contact [book.department@intechopen.com](mailto:book.department@intechopen.com)

Numbers displayed above are based on latest data collected.

For more information visit [www.intechopen.com](http://www.intechopen.com)



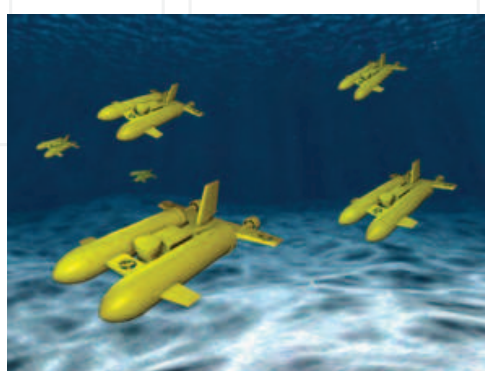
# Short-Range Underwater Acoustic Communication Networks

Gunilla Burrowes and Jamil Y. Khan  
The University of Newcastle  
Australia

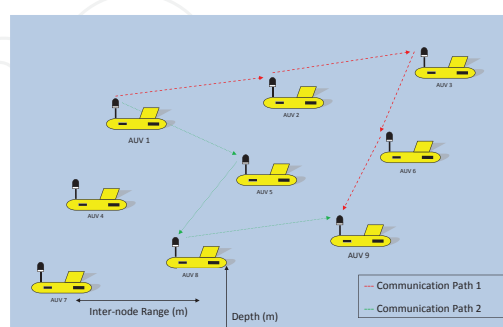
## 1. Introduction

This chapter discusses the development of a short range acoustic communication channel model and its properties for the design and evaluation of MAC (Medium Access Control) and routing protocols, to support network enabled Autonomous Underwater Vehicles (AUV). The growth of underwater operations has required data communication between various heterogeneous underwater and surface based communication nodes. AUVs are one such node, however, in the future, AUV's will be expected to be deployed in a swarm fashion operating as an ad-hoc sensor network. In this case, the swarm network itself will be developed with homogeneous nodes, that is each being identical, as shown in Figure 1, with the swarm network then interfacing with other fixed underwater communication nodes. The focus of this chapter is on the reliable data communication between AUVs that is essential to exploit the collective behaviour of a swarm network.

A simple 2-dimensional (2D) topology, as shown in Figure 1(b), will be used to investigate swarm based operations of AUVs. The vehicles within the swarm will move together, in a decentralised, self organising, ad-hoc network with all vehicles hovering at the same depth. Figure 1(b) shows the vehicles arranged in a 2D horizontal pattern above the ocean floor



(a) AUV Swarm demonstrating stylised SeaVision©vehicles



(b) 2D AUV Swarm Topology

Fig. 1. Swarm Architecture

giving the swarm the maximum coverage area at a single depth, while forming a multi-hop communication network. The coverage area will depend on application. For example, the exploration of oil and gas deposits underwater using hydrocarbon sensing would initially require a broad structure scanning a large ocean footprint before narrowing the range between vehicles as the sensing begins to target an area. Thus vehicles may need to work as closely as 10 m with inter-node communication distance extending out to 500 m. These operating distances are substantially shorter than the more traditional operations of submarines and underwater sensor to surface nodes that have generally operated at greater than 1km. Thus, the modelling and equipment development for the communication needs of these operations has focused on longer range data transmission and channel modelling. To exploit the full benefits of short range communication systems it is necessary to study the properties of short range communication channels.

Most AUV development work has concentrated on the vehicles themselves and their operations as a single unit (Dunbabin et al., 2005; Holmes et al., 2005), without giving much attention to the development of the swarm architecture which requires wireless communication networking infrastructure. To develop swarm architectures it is necessary to research effective communication and networking techniques in an underwater environment. Swarm operation has many benefits over single vehicle use. The ability to scan or 'sense' a wider area and to work collaboratively has the potential to vastly improve the efficiency and effectiveness of mission operations. Collaboration within the swarm structure will facilitate improved operations by building on the ability to operate as a team which will result in emergent behaviours that are not exhibited by individual vehicles. A swarm working collaboratively can also help to mitigate the problem of high propagation delay and lack of bandwidth available in underwater communication environments. Swarm topology will facilitate improved communication performance by utilising the inherent spatial diversity that exists in a large structure. For example, information can be transmitted more reliably within a swarm architecture by using multi-hop networking techniques. In such cases, loss of an individual AUV, which can be expected at times in the unforgiving ocean environment, will have less detrimental effect compared to a structure where multiple vehicles operate on their own. (Stojanovic, 2008).

The underwater acoustic communication channel is recognised as one of the harshest environments for data communication, with long range calculations of optimal channel capacity of less than 50kbps for SNR (Signal-to-Noise Ratio) of 20dB (Stojanovic, 2006) with current modem capacities of less than 10kbps (Walree, 2007). Predictability of the channel is very difficult with the conditions constantly changing due to seasons, weather, and the physical surroundings of sea floor, depth, salinity and temperature. Therefore, it must be recognised that any channel model needs to be adaptable so that the model can simulate the channel dynamics to be able to fully analyse the performance of underwater networks.

In general, the performance of an acoustic communication system underwater is characterised by various losses that are both range and frequency dependent, background noise that is frequency dependent and bandwidth and transmitter power that are both range dependent. The constraints imposed on the performance of a communication system when using an acoustic channel are the high latency due to the slow speed of the acoustic signal propagation, at 0.67 ms/m (compared with RF (Radio Frequency) in air at 3.3 ns/m), and the signal fading properties due to absorption and multipath. Specific constraints on the performance due to the mobility of AUV swarms is the Doppler effect resulting from any relative motion between

a transmitter and a receiver, including any natural motion present in the oceans from waves, currents and tides.

Noise in the ocean is frequency dependent. There are three major contributors to noise underwater: ambient noise which represents the noise in the far field; self noise of the vehicle (considered out of band noise); and intermittent noise sources including noises from biological sources such as snapping shrimp, ice cracking and rain. Ambient noise is therefore the component of noise taken into account in acoustic communication performance calculations. It is characterised as a Gaussian Distribution but it is not white as it does not display a constant power spectral density. For the frequencies of interest for underwater acoustic data communication, from 10 to 100 kHz, the ambient noise value decreases with increasing frequency. Therefore, using higher signal frequencies, which show potential for use in shorter range communication, will be less vulnerable to the impact of ambient noise.

Short range underwater communication systems have two key advantages over longer range operations; a lower end-to-end delay and a lower signal attenuation. End-to-end propagation at 500 m for example is approximately 0.3 sec which is considerable lower than the 2 sec at 3 km but still critical as a design parameter for shorter range underwater MAC protocols. The lower signal attenuation means potentially lower transmitter power requirements which will result in reduced energy consumption which is critical for AUVs that rely on battery power. Battery recharge or replacement during a mission is difficult and costly. The dynamics associated with attenuation also changes at short range where the spreading component dominates over the absorption component, which means less dependency on temperature, salinity and depth (pressure). This also signifies less emphasis on frequency as the frequency dependent part of attenuation is in the absorption component and thus will allow the use of higher signal frequencies and higher bandwidths at short ranges. This potential needs to be exploited to significantly improve the performance of an underwater swarm network communication system.

A significant challenge for data transmission underwater is multipath fading. The effect of multipath fading depends on channel geometry and the presence of various objects in the propagation channel. Multipath's occur due to reflections (predominately in shallow water), refractions and acoustic ducting (deep water channels), which create a number of additional propagation paths, and depending on their relative strengths and delay values can impact on the error rates at the receiver. The bit error is generated as a result of inter symbol interference (ISI) caused by these multipath signals. For very short range single transmitter-receiver systems, there could be some minimisation of multipath signals (Hajenko & Benson, 2010; Waite, 2005). For swarm operations, however, there is potentially a different mix of multipath signals that need to be taken into account, in particular, those generated due to the other vehicles in the swarm.

Careful consideration of the physical layer parameters and their appropriate design will help maximise the advantages of a short range communications system that needs to utilise the limited resources available in an underwater acoustic networking environment.

The following section will introduce the parameters associated with acoustic data transmission underwater. The underwater data transmission channel characteristics will be presented in Section 3 with a discussion of the advantages and disadvantages of the short range channel. Section 4 will show how these will impact on AUV swarm communications and the development of a short range channel model for the design and evaluation of MAC and routing protocols. This is followed in Section 5 by a discussion of the protocol techniques required for AUV swarm network design.

## 2. Introduction to acoustic underwater communication network

The underwater data communication link and networking environment presents a substantially different channel to the RF data communication channel in the terrestrial atmosphere. Figure 2 illustrates a typical underwater environment for data transmission using a single transmitter-receiver pair.

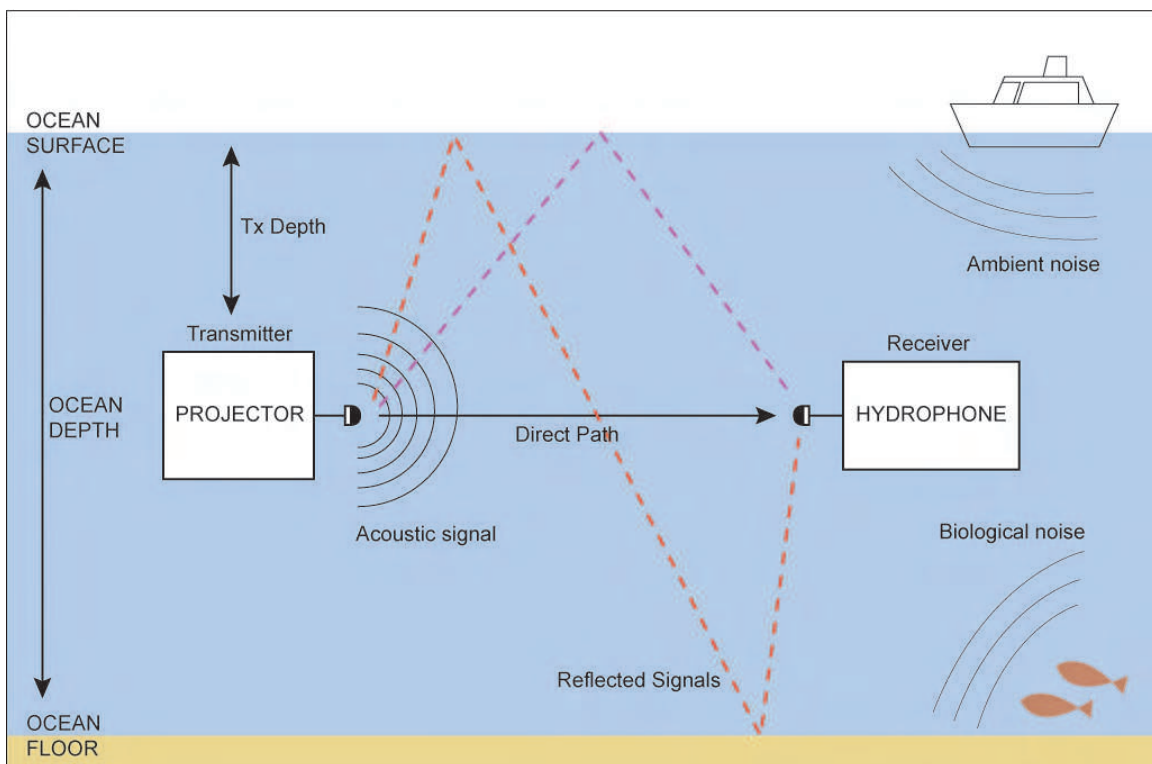


Fig. 2. Underwater Acoustic Environment

A simple schematic of the data transmission scheme involving a projector (transmitter) and a hydrophone (receiver) is presented in Figure 3. The projector takes the collected sensor and navigational data and formats it into packets at the Data Source and this is then modulated with the carrier frequency. The modulated signal is amplified to a level sufficient for signal reception at the receiver. There is an optimum amplification level as there is a trade-off between error free transmission and conservation of battery energy. The acoustic power radiated from the projector as a ratio to the electrical power supplied to it, is the efficiency  $\eta_{tx}$  of the projector and represented by the Electrical to Acoustic conversion block. On the receiver side, the sensitivity of the hydrophone converts the sound pressure that hits the hydrophone to electrical energy, calculated in dB/V. Signal detection, includes amplification and shaping of the input to determine a discernible signal. Here a detection threshold needs to be reached and is evaluated as the ratio of the mean signal power to mean noise power (SNR). The carrier frequency is then supplied for demodulation, before the transmitted data is available for use within the vehicle for either data storage or for input into the vehicles control and navigation requirements.

Underwater data communication links generally support low data rates mainly due to the constraints of the communication channel. The main constraints are the high propagation delay, lower effective SNR and lower bandwidth. The effects of these constraints could be reduced by using short distance links and the use of multi-hop communication techniques to

cover longer transmission ranges. For an AUV swarm network, use of the above techniques could be crucial to design an effective underwater network. To develop a multi-node swarm network it is necessary to manage all point to point links using a medium access control (MAC) protocol. In a multi-access communication system like a swarm network a transmission channel is shared by many transceivers in an orderly fashion to transmit data in an interference free mode. Figure 2 shows a point to point communication link with two AUVs. When a network is scaled up to support N number of AUVs then it becomes necessary to control multiple point to point or point to multi-point links.

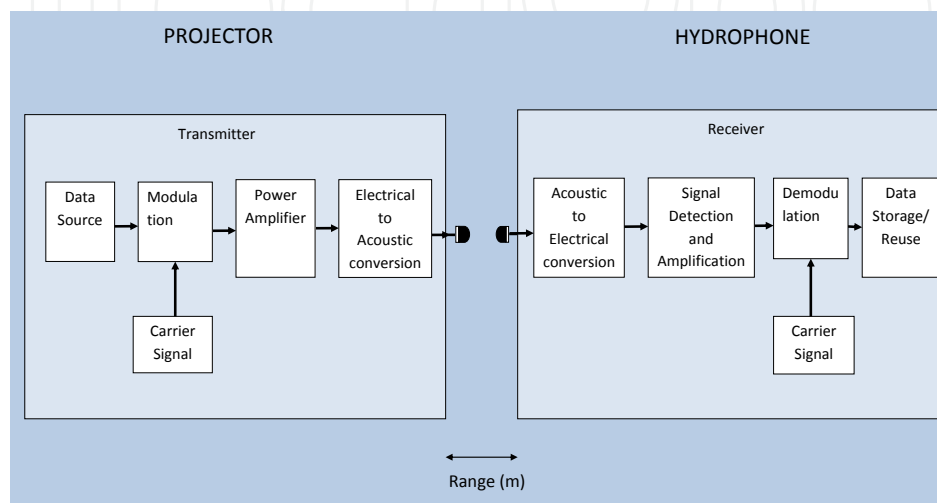


Fig. 3. Block Diagram of Projector and Hydrophone

To control the transmission of data it is necessary to design an effective MAC protocol which can control transmission of information from different AUVs. The design of a MAC protocol in a swarm network could be more complex if a multi-hop communication technique is used. The multi-hop communication technique will allow a scalable network design as well as it can support long distance transmission without the need of high power transmitter and receiver circuits. For example, using a multi-hop communication technique if AUV3 in Figure 1(b) wants to transmit packets to AUV7 then it can potentially use a number of communication paths to transmit packets. Some of the possible paths from AUV3 to AUV7 are: AUV3-AUV2-AUV1-AUV4-AUV7 or AUV3-AUV6-AUV9-AUV8-AUV7. The path selection in a network is controlled by the routing protocols. Optimum routing protocols generally select transmission paths based on a number of factors. However, the main factor used to select an optimum path in a wireless network is the SNR which indicates the quality of a link. Similarly the MAC protocol will use the transmission channel state information to develop an optimum packet access technique. To effectively design these protocols it is necessary to understand the properties of short range underwater channel characteristics. Before moving into the protocol design issues we will first evaluate the short range underwater channel characteristics in the following Sections.

### 3. Underwater data transmission channel characteristics

This section will focus on the parameters of the ocean channel that will affect the acoustic signal propagation from the projector to the hydrophone. There are well established

underwater channel models that will be used to derive and present the data transmission characteristics for a short-range link.

### 3.1 Acoustic signal level

The projector source level,  $SL_{tprojector}$ , is generally defined in terms of the sound pressure level at a reference distance of 1 m from its acoustic centre. The source intensity at this reference range is  $I = P_{tx} / Area$  ( $W/m^2$ ) and measured in dB 're 1  $\mu Pa$ ' but strictly meaning 're the intensity due to a pressure of 1  $\mu Pa$ '. For an omni directional projector the surface area is a sphere ( $4\pi r^2 = 12.6m^2$ ). Thus,  $SL_{projector} = 10\log((P_{tx}/12.6)/I_{ref})$  dB, where  $P_{tx}$  is the total acoustic power consumed by projector and the reference wave has an intensity:  $I_{ref} = (Pa_{ref})^2 / \rho * c$  ( $Wm^{-2}$ ) where reference pressure level;  $Pa_{ref}$  is 1  $\mu Pa$ ,  $\rho$  is the density of the medium and;  $c$  is the speed of sound (averages for sea water:  $\rho = 1025 kg/m^3$  and  $c=1500 m/s$ ) (Coates, 1989; Urick, 1967).

The equation for the transmitter acoustic signal level ( $SL_{projector}$ ) at 1 m for an omni-directional projector can be written:

$$SL_{projector}(P) = 170.8 + 10\log P_{tx} \quad dB \quad (1)$$

If the projector is directional, then the projector directivity index is  $DI_{tx} = 10\log(\frac{I_{dir}}{I_{omni}})$  where  $I_{omni}$  is the intensity if spread spherically and  $I_{dir}$  is the intensity along the axis of the beam pattern. Directivity can increase the source level by 20dB (Waite, 2005). The more general equation for the transmitter acoustic signal level ( $SL_{projector}$ ) can be written:

$$SL_{projector}(P, \eta, DI) = 170.8 + 10\log P_{tx} + 10\log \eta_{tx} + DI_{tx} \quad dB \quad (2)$$

where the efficiency of the projector  $\eta_{tx}$  takes into account the losses associated with the electrical to acoustic conversion as shown in Figure 3, thus reducing the actual SL radiated by the projector. This efficiency is bandwidth dependent and can vary from 0.2 to 0.7 for a tuned projector (Waite, 2005).

### 3.2 Signal attenuation

Sound propagation in the ocean is influenced by the physical and chemical properties of seawater and by the geometry of the channel itself. An acoustic signal underwater experiences attenuation due to spreading and absorption. In addition, depending on channel geometry multipath fading may be experienced at the hydrophone. Path loss is the measure of the lost signal intensity from projector to hydrophone. Understanding and establishing an accurate path loss model is critical to the calculations of Signal-to-Noise ratio (SNR).

#### 3.2.1 Spreading loss

Spreading loss is due to the expanding area that the sound signal encompasses as it geometrically spreads outward from the source.

$$PL_{spreading}(r) = k * 10\log(r) \quad dB \quad (3)$$

where  $r$  is the range in meters and  $k$  is the spreading factor.

When the medium in which signal transmission occurs is unbounded, the spreading is spherical and the spreading factor  $k=2$  whereas in bounded spreading, considered as cylindrical  $k=1$ . Urick (1967) suggested that spherical spreading was a rare occurrence in the ocean but recognised it may exist at short ranges. As AUV swarm operations will occur

at short range it is likely that spherical spreading will need to be considered which means a higher attenuation value. Spreading loss is a logarithmic relationship with range and its impacts on the signal is most significant at very short range up to approximately 50m as seen in Figure 5(a). At these shorter ranges spreading loss plays a proportionally larger part compared with the absorption term (which has a linear relationship with range).

### 3.2.2 Absorption loss

The absorption loss is a representation of the energy loss in the form of heat due to the viscous friction and ionic relaxation that occurs as the wave generated by an acoustic signal propagates outwards and this loss varies linearly with range as follows:

$$PL_{absorption}(r, f) = 10 \log(\alpha(f)) * r \quad dB \quad (4)$$

where  $r$  is range in kilometres and  $\alpha$  is the absorption coefficient.

More specifically the absorption of sound in seawater is caused by three dominant effects; viscosity (shear and volume), ionic relaxation of boric acid and magnesium sulphate ( $MgSO_4$ ) molecules and the relaxation time. The effect of viscosity is significant at high frequencies above 100 kHz, whereas the ionic relaxation effects of magnesium affect the mid frequency range from 10 kHz up to 100 kHz and boric acid at low frequencies up to a few kHz. In general, the absorption coefficient,  $\alpha$ , increases with increasing frequency and decreases as depth increases (Domingo, 2008; Sehgal et al., 2009) and is significantly higher in the sea compared with fresh water due predominately to the ionic relaxation factor.

Extensive measurements of absorption losses over the last half century has lead to several empirical formulae which take into account frequency, salinity, temperature, pH, depth and speed of sound. A popular version is Thorp's expression (Thorp, 1965), Equation 5, which is based on his initial investigations in the 60's and has since been converted into metric units (shown here). It is valid for frequencies from 100Hz to 1MHz and is based on seawater with salinity of 35% ppt, pH of 8, temp of 4°C and depth of 0 m (atmospheric pressure) which is assumed but not stated by Thorp.

$$\alpha(f) = \frac{0.11f^2}{1 + f^2} + \frac{44f^2}{4100 + f^2} + 2.75 \times 10^{-4}f^2 + 0.0033 \quad dB/km \quad (5)$$

Fisher and Simmons (1977) and others (Francois & Garrison, 1982) have since proposed other variations of  $\alpha$ . In particular, Fisher and Simmons in the late 70's found the effect associated with the relaxation of boric acid on absorption and provided a more detailed form of absorption coefficient  $\alpha$  in dB/km which varies with frequency, pressure (depth) and temperature (also valid for 100 Hz to 1 MHz with salinity 35% ppt and acidity 8 pH)(Fisher & Simmons, 1977; Sehgal et al., 2009), given in Equation 6.

$$\alpha(f, d, t) = \frac{A_1 f_1 f^2}{f_1^2 + f^2} + \frac{A_2 P_2 f_2 f^2}{f_2^2 + f^2} + A_3 P_3 f^2 \quad dB/km \quad (6)$$

where  $d$  is depth in meters and  $t$  is temperature in °C. The 'A' coefficients represent the effects of temperature, while the 'P' coefficients represent ocean depth (pressure) and  $f_1, f_2$  represent the relaxation frequencies of Boric acid and ( $MgSO_4$ ) molecules. These terms were developed by Fisher and Simmons (1977) and presented more recently by (Domingo, 2008; Sehgal et al., 2009).



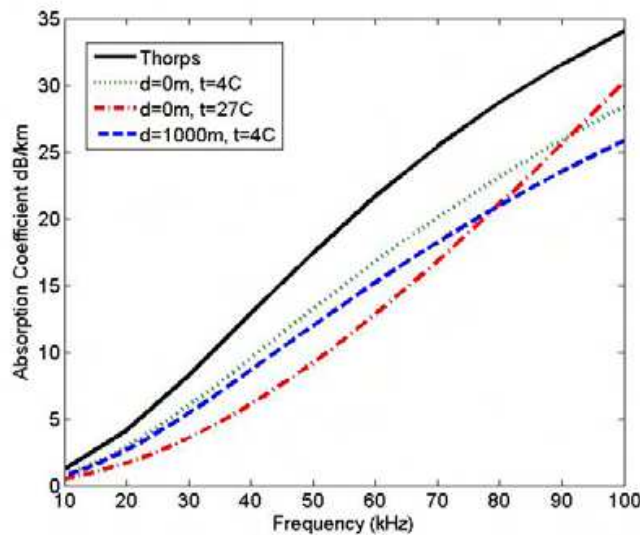


Fig. 4. Absorption Coefficient vs Frequency

Figure 4 shows the absorption coefficients in dB/km vs signal frequency for both Thorp and Fisher and Simmons coefficients and shows that in general  $\alpha$  increases with increasing frequency at any fixed temperature and depth. Up until around 80kHz temperature change has a more significant affect on  $\alpha$  than depth (Waite, 2005), but above these frequencies depth begins to dominate (Domingo, 2008; Sehgal et al., 2009). In any case, Thorps 'approximation' is quite close to Fisher and Simmons and is clearly more conservative at the frequencies shown. Sehgal (2009) shows that at higher frequencies above 300kHz, Thorps model predicts lower losses as it does not take into account the relaxation frequencies found by Fisher and Simmons. If depth and frequency are fixed and temperature varied from 0 to 27 °C, there is a decrease in  $\alpha$  of approximately 4 dB/km for frequencies in the range of 30 to 60kHz which correlates to work presented by Urick (Urick, 1967)(Fig5.3 pg 89). If we consider where AUV swarms are most likely to operate, in the 'mixed surface layer', where temperature varies considerable due to latitude (but has an average temp of 17°C (Johnson, 2011)), temperature may be an important factor. It should be noted that if operating in lower temperatures  $\alpha$  is higher and thus using 0°C will be a conservative alternative. At shorter ranges, the significance of  $\alpha$  is expected to be less due to the linear relationship with range which will be discussed further in this chapter.

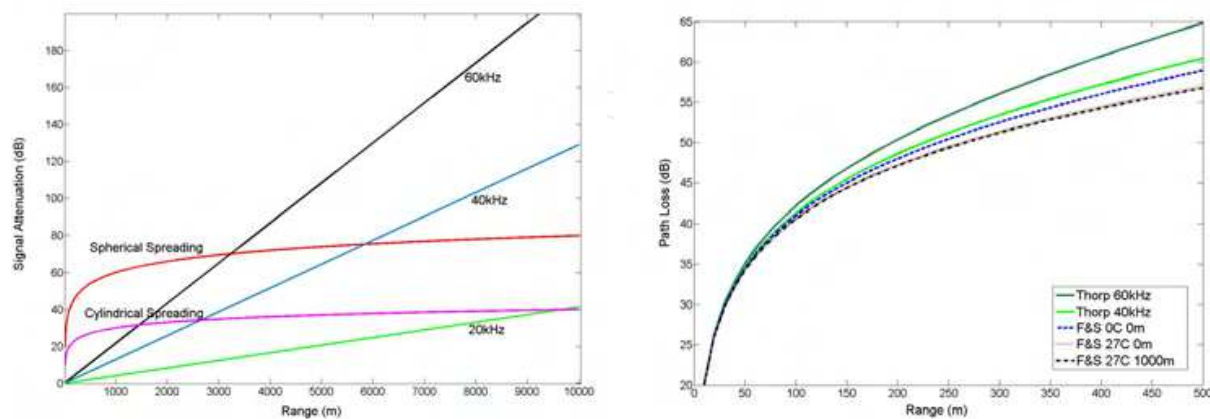
As mentioned, depth (pressure) has less of an effect on  $\alpha$  than temperature at these lower frequencies. Domingo (Domingo, 2008) investigates the effect of depth (pressure) on absorption and confirms that for lower frequencies of less than 100kHz there is less change in  $\alpha$ . More specifically Urick (1967) defined the variation by:  $\alpha_d = \alpha * 10^{-3}(1 - 5.9 * 10^{-6}) * d$  dB/m (where d = depth in meters) but has also suggested an approximation of a 2% decrease for every 300 m depth. Thus, depth (pressure) variations are not expected to play a significant role in short range AUV swarm operations especially those that use a 2D horizontal topology as described in this chapter.

### 3.3 Path loss

Total path loss is the combined contribution of both the spreading and absorption losses. Urick (1967) established that this formula of spreading plus absorption yields a reasonable

agreement with long range observations.

$$PathLoss(r, f, d, t) = k * 10\log(r) + \alpha(f, d, t) * r * 10^{-3} \quad (7)$$



(a) Signal Attenuation showing spherical spreading and absorption factors (b) Comparing Absorption Models using spherical spreading. Frequency change shown using Thorp Model and Temperature  $^{\circ}C$  and Depth  $'m'$  changes shown in Fisher and Simmons Model.

Fig. 5. Path Loss vs Range

For very short range communication (below 50 m), see Figure 5(a), the contribution of the absorption term is less significant than the spreading term. It can be seen in Figure 5(b) that the Thorp model shows a conservative or worst case value for the ranges of interest up to 500 m. The Fisher and Simmons model for a particular frequency however provides some insight into the variations due to depth and temperature. However, the spreading factor  $k$  has the most significant affect on Path Loss, seen in Figure 5(a), at these shorter ranges according to these models.

As range increases and the absorption term begins to dominate, any variations in  $\alpha$  also becomes more significant. For data communication, the changes in the attenuation due to signal frequency are particularly important as the use of higher frequencies will potentially provide higher data rates.

In summary using the two models, Thorp and Fisher and Simmons, the two important characteristics that can be drawn from Path Loss at the short ranges of interest for AUV swarm operation are:

- spreading loss dominates over absorption loss, and thus the ' $k$ ' term has a significant impact on the attenuation of the signal at shorter ranges as illustrated in Figure 5 (a). For AUV swarm operations and while the range between vehicles is much less than depth spherical spreading can be assumed, and
- at the ranges below 500 m the frequency component of absorption loss is most significant compared with the possible temperature and pressure (depth) changes as seen in Figure 5(b) and as range increases the difference also increases, effectively meaning that the communication channel is band-limited and available bandwidth is a decreasing function of range.

### 3.4 Underwater multipath characteristics

Multipath signals, in general, represent acoustic energy loss, however, for communication systems it is the Inter Symbol Interference (ISI) that will also be detrimental at the receiver as it can significantly increase the error rate of the received signal. Multipath signals are created underwater through various mechanisms described in this section, so that, at the receiver many components of the original signal will arrive at different times due to the different length of propagation paths the multipath signals have taken. It is this delay spread of the signal component arrivals that can cause ISI to occur if they overlap with previous or future signal arrivals which will cause symbol corruption or loss and therefore bit errors. As the speed of sound propagation is very slow in an acoustic channel this delay spread can be significant.

There are two major mechanisms responsible for creating multi-path signals and these are: reverberation, which refers to the reflections and scattering of the sound signal; and ray bending, which is a result of the unique sound speed structure in the oceans which create temperature gradient channels that trap acoustic signals. Multi-path signal formation is therefore determined by the geometry of the channel in which transmission is taking place, the location of the transmitter and receiver, and importantly the depth at which it is occurring. In shallow water, multi-path is due predominately to reverberation whereas in deep water it is dominated by ray bending, although reverberation will occur in deep water if the transmitter and receiver are located near the surface or bottom (Coates, 1989; Domingo, 2008; Etter, 2003; Urlick, 1967).

There are several physical effects which create reverberation underwater;

- Multi-path propagation caused by boundary reflections at the sea-floor or sea-surface, seen in Figure 2.
- Multi-path propagation caused by reflection from objects suspended in the water, marine animals or plants or bubbles in the path of the transmitted signal
- Surface scattering caused by sea-surface (waves) or sea-floor roughness or surface absorption, particularly on the sea bottom depending on material
- Volume scattering caused by refractive off objects suspended in the signal path

Ray bending, causes various propagation path loss mechanisms in deep water depending on the placement of transmitter and receivers. The propagating acoustic signal bends according to Snell's Law, to lower signal speed zones. Figure 6 shows a typical ocean Sound Speed Profile, although variations occur with location and seasons. The profile is depth dependent, where sound speed is influenced more by temperature in the surface layers and by pressure at greater depths.

The various path loss mechanisms include; (Domingo, 2008)

- Surface duct, Figure 7(a) occurs when the surface layer has a positive temperature gradient, the acoustic signals can bend back towards the surface, then reflect back into the layer off the surface
- Deep Sound Channel, sometimes referred to as the SOFAR (Sound Fixing and Ranging) channel, where acoustic propagation occurs above and below the level of minimum sound speed, when the sound rays continually are bent towards the depth of minimum speed, shown in Figure 7(a)
- Convergence zone, in deep water areas when the transmitter is located quite close to the surface and the sound rays bend downwards as a result of decreasing temperatures until the increase in pressure forces the rays back towards the surface, as shown in Figure 7(b)

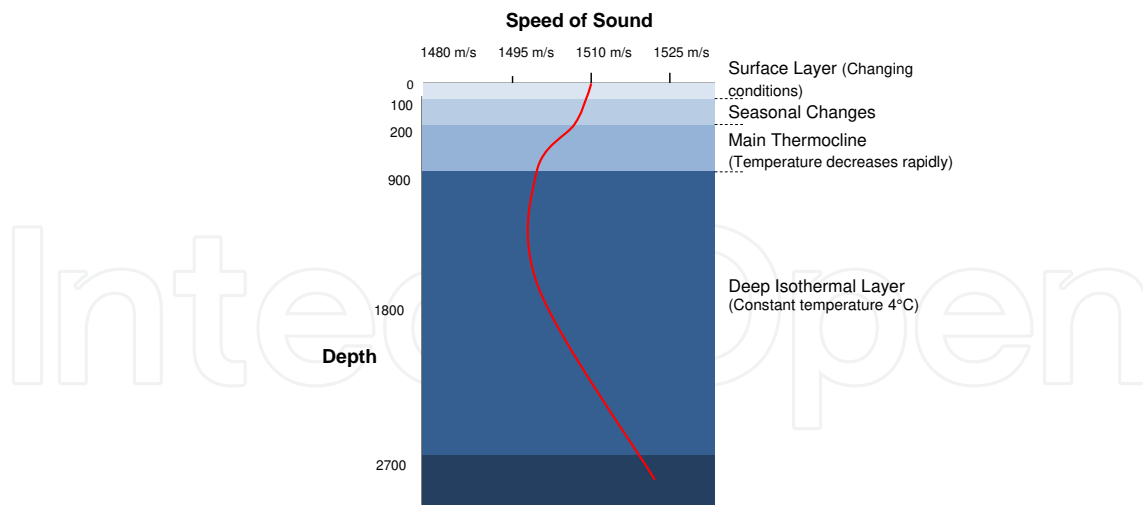
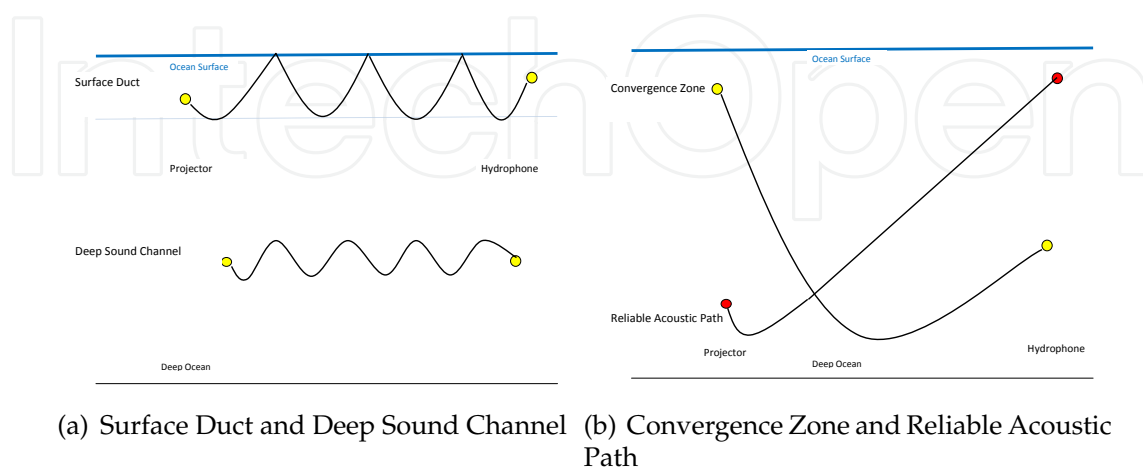


Fig. 6. Typical Sound Speed Profile in the Ocean Cox (1974)

- Reliable acoustic path, which occurs when the transmitter is located in very deep water and receiver in shallow water. Referred to as reliable as it is not generally affected by bottom or surface reflections, as shown in Figure 7(b) and
- Shadow zones that are considered a special case, as these 'zones' are void from any signal propagation. This means that in Shadow zones a hydrophone may not receive any signal at all.

Thus the geometry of the channel being used is a major determinate of the number of significant propagation paths and their relative strengths and delays. Apart from the Shadow Zones where no signal or multipath components of the signal can reach the hydrophone, the hydrophone may receive the direct signal and a combination of various multipath signals that have been reflected, scattered or bent. It is these multiple components of the signal that are delayed in time due to the various path lengths that may create ISI and errors in symbol detection.



(a) Surface Duct and Deep Sound Channel (b) Convergence Zone and Reliable Acoustic Path

Fig. 7. Ray Bending Path Loss Mechanisms

For very short range channels that will be used in AUV swarm operations, multipath will be influenced also by the range-depth ratio, which is expected to produce fewer multipath signals at the hydrophone (Hajenko & Benson, 2010; Parrish et al., 2007). In addition some improvement can be gained through directing the beam of the transmitted signal and the directional properties of the receiver (Essebbar et al., 1994), however this will require an additional level of complexity for mobile AUV's due to the need for vehicle positioning before sending or when receiving a signal.

Most of the discussion so far has focused on time-invariant acoustic channel multipath where deterministic propagation path models have been developed for the various reflective and ray bending path options. These are significant in themselves with multipath spreads in the order of 10 to 100 ms. Take Figure 2, where projector and hydrophone are separated by 100m and are at a depth of 100m, the delay spread between the direct path and the first surface reflection is  $\approx 28$  ms. Multipath in an underwater channel, however, also has time-varying components caused by the surface or volume scattering or by internal waves in deep water that are responsible for random signal fluctuations. Unlike in radio channels, the statistical characterisation of these random processes in the underwater channel are in their early development stages. Experimental results have shown that depending on the day, the location and the depth of communication link, the results of multipath can follow one of the deterministic models discussed here to worst case coherence times in the order of seconds (Stojanovic, 2006). Another source of time variability in an underwater communication channel occurs when there is relative motion between the transmitter and receiver as will be briefly discussed in the following sub-section.

### 3.5 The doppler effect

The motion of AUV's relative to each other will cause two possible forms of Doppler distortion in the received signal, Doppler Shifting caused by an apparent shift in frequency as the vehicles move towards or away from each other and Doppler Spreading or its time domain dual coherence time, which is the measure of the time varying nature of the frequency dispersiveness in the doppler spectrum (Rappaport, 1996). The doppler shift ( $\Delta f$ ) of a received signal is  $f_c \frac{\Delta v}{c}$  where  $f_c$  is the original signal frequency and  $\Delta v$  is the relative velocity between the moving vehicles. As an example, if the vehicles were moving at a moderately slow speed of 1 m/s (2 knots) relative to each other and  $f_c = 40kHz$  the  $\Delta f \approx 27Hz$ . Doppler spread or coherence time measurements as mentioned above can be as long as 1 s. Thus doppler shifting and spreading cause complications for the receiver to track the time varying changes in the channel which need to be designed into the channel estimation algorithms and explicit delay synchronisation approach within communication protocols. As swarm operations for exploration require rigid topology where there is minimal relative speed differences between vehicles, the impact of doppler effects diminished somewhat in this context and thus will not be considered further.

### 3.6 Noise

There are three major contributors to noise underwater: ambient or background noise of the ocean; self noise of the vehicle; and intermittent noise including biological noises such as snapping shrimp, ice cracking and rain. An accurate noise model is critical to the evaluate the SNR at the hydrophone so that the bit error rates (BER) can be establish to evaluate protocol performance.

### 3.6.1 Ambient noise

Ambient Noise in the ocean has been well defined (Urick, 1967). It can be represented as Gaussian and having a continuous power spectrum density (psd). It is made up of four components (outlined below), each having a dominating influence in different portions of the frequency spectrum.

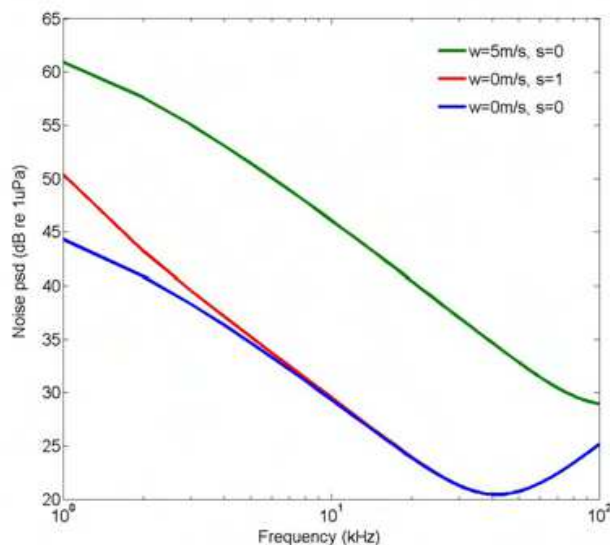


Fig. 8. Power Spectral density of the Ambient Noise, W - wind, S - shipping

For the frequency region of interest for AUV swarm communication systems (10 kHz to 100 kHz), the ambient noise psd decreases with increasing frequency, refer to Figure 8. At a frequency over 100kHz the ambient thermal noise component begins to dominate and the overall noise psd begins to increase, but this point moves further away from the frequencies of interest for AUV communication particularly as the wind speed increases.

- Turbulence noise influences only the very low frequency regions  $f < 10\text{Hz}$   
 $10\log N_{turb}(f) = 17 - 30\log(f)$
- Shipping noise dominates the 10 - 100Hz region and has defined a shipping activity factor of  $s$  whose value ranges from 0 to 1 for low to high activity respectively:  
 $10\log N_{ship}(f) = 40 + 20(s - 0.5) + 26\log(f) - 60\log(f + 0.03)$
- Wave and other surface motion caused by wind and rain is a major factor in the mid frequency region of 100Hz - 100kHz where wind speed is given by  $w$  in m/s:  
 $10\log N_{wind}(f) = 50 + 7.5w^{1/2} + 20\log(f) - 40\log(f + 0.4)$
- Thermal noise becomes dominate over 100kHz:  
 $10\log N_{th}(f) = -15 + 20\log(f)$

where wind speed is given by  $w$  in m/s (1m/s is approximately 2 knots) and  $f$  is in kHz. Ambient Noise power also decreases with increasing depth as the distance from the surface and therefore shipping and wind noise becomes more distant. Ambient noise has been shown to be 9dB higher in shallow water than deep water (Caruthers, 1977). Swarm operations, as well as other underwater networking operations will mean that communication nodes including AUV's will be working in relatively close proximity to other nodes which will add an additional level of ambient noise to their operations due to the noise of the other vehicles in

the swarm, irrespective of the operating depth. As will be discussed in the next section on Self Noise, the expectation is that this additional 'ambient noise' which relates to the 'Shipping Noise' component of ambient noise will have limited affect on the acoustic communication which generally uses frequencies above 10kHz.

### 3.6.2 Self noise

Self noise is defined as the noise generated by the vehicle itself as the platform for receiving signals. This noise can reach the hydrophone mounted on the AUV either through the mechanical structure or through the water passing over the hydrophone. The degree to which turbulent flows cause transducer self noise depends on the location (mounting) of the transducer and its directivity characteristics (Sullivan & Taroudakis, 2008). Self Noise can also be seen as an equivalent isotropic noise spectrum as presented by Urick from work done during WWII on submarines. In general, as with ambient noise, there is decreasing levels of self noise with increases in frequency however self noise is also significantly affected by speed with decreasing noise spectra when the vessels are travelling at slower speeds or are stationary (Eckart, 1952; Kinsler et al., 1982; Urick, 1967).

Kinsler (1982) notes that at low frequencies (<1kHz) and slow speeds machinery noise dominates and at very slow speeds self noise is usually less important than ambient noise. Whereas at higher frequencies (10kHz) propeller and flow noise begins to dominate and as speed increases the hydrodynamic noise around the hydrophone increases strongly and becomes more significant than the machinery noise. This is due to the cavitation from the propeller due to the entrainment of air bubbles under or on the blade tip of the propeller. At higher speeds, self noise can be much more significant than ambient noise and can become the limiting factor.

The self noise of different size and types of vehicles are as varied as there are vehicle designs and there is little recent published values. Each vehicle itself produces large variations in self noise with speed and operating conditions (Eckart, 1952). Self noise can be controlled by selection of motor type, configuration, mounting and motor drivers. The trend for most AUV's will be the use of small brush-less DC electric motors which have been used on the development of the SeaVision vehicle (Mare, 2010). Preliminary testing of self noise on these vehicles shows an increase in noise due to increases in speed, as has been predicted, but there was no way to distinguish between machinery and hydrodynamic affects. Higher frequency components (up to 20kHz) were present as the speed increased due to the increased work from the thrusters. When the SeaVision vehicle hovered in a stationary position the frequency of the noise psd centred around 2kHz, which is out of band noise.

Holmes (Holmes et al., 2005) at WHOI recently investigated the self noise of REMUS, their torpedo shape AUV, used as a towed array. At the maximum RPM of the AUV, the 1/3rd octave noise level, when converted to source level by the calibrated transmission factor, was 130 dB re  $1\mu Pa$  at 1m directly aft of the vehicle for a centre frequency of 1000 Hz. This would represent the radiated noise source level for a vehicle moving at 3 knots (1.5m/s). Vehicles typically radiate less noise in free operating conditions than in tethered conditions, so the second trail on the REMUS was measuring the radiated noise of the vehicle to examine the power spectral density of the noise as recorded on the hydrophone array as it was towed behind the vehicle. The results showed the RPM dependent radiated noise in the aft direction at a distance of 14.6 m behind the vehicle looking at frequency range up to 2500Hz which is again out of band noise.

As the operating frequencies of the communication system is likely to be higher than most self noise, and the vehicles will operate relatively slowly, the expected contribution of self noise on the hydrophone reception will be low.

### 3.6.3 Intermittent sources of noise

The sources of intermittent noise can become very significant in locations or times that they occur close to operating AUV swarms. The two major areas where research has been undertaken are in the marine bio-acoustic fields and also the effect of rain and water bubbles created by raindrops.

Major contributors to underwater bio-acoustic noise include;

- Shellfish - Crustacea - most important here are the snapping scrimp who produce a broad spectrum of noise between 500Hz and 20kHz
- Fish - toadfish 10 to 50Hz
- Marine mammals - Cetacea - porpoises 20 to 120Hz

Rain creates different noise spectrum to wind and needs to be dealt with separately as it is not a constant source of noise. Urick (1967) showed examples of increases of almost 30dB in the 5 to 10kHz portion of spectrum in heavy rain, with steady rain increasing noise by 10dB or sea state equivalent increase from 2 to 6. Eckart (1952) presented average value of rain at the surface from 100Hz to 10kHz of -17 to 9dB.

These main contributors to intermittent sources predominate in the lower frequency ranges up to 20kHz. Thus, interference in the operating frequencies of communication data signals is considered low.

## 4. Short range channel modelling

Utilising the full capacity of the underwater acoustic channel is extremely important as the channel exhibits such challenging and limited resources as has been discussed. For short range data transmission operations there are a number of benefits that can be gained over current longer range underwater acoustic transmission. These will now be explored further in terms of data communication protocol design and development. In particular, finding the optimum signal frequency and bandwidth at different ranges and under various channel conditions will be evaluated on the basis of using the best Signal-to-Noise ratio (SNR) possible at the hydrophone. Investigation into channel capacity and BER for various possible modulation schemes will also be analysed to set up the background to the challenges for MAC and routing protocol design.

### 4.1 Frequency dependent component of SNR

The narrowband Signal-to-Noise-Ratio (SNR) observed at the receiver, assuming no multi-path or doppler losses is given by:

$$SNR(r, f, d, t, w, s, P_{tx}) = \frac{SL_{projector}(P_{tx}, \eta, DI)}{PathLoss(r, f, d, t) \sum Noise(f, w, s) \times B} \quad (8)$$

where B is the receiver bandwidth and the Signal Level (SL), PathLoss and Noise terms have been previously developed.

Taking the frequency dependent portion of the SNR from Equation 8, as developed by Stojanovic (2006), is the  $PathLoss(r, f, d, t) \sum Noise(f, w, s)$  product. Since SNR is inversely



proportional to  $PathLoss(r, f, d, t) \sum Noise(f, w, s)$  factor, the  $\frac{1}{PathLoss(r, f, d, t) Noise(f, w, s)}$  term is illustrated in the Figures 9 (a) for longer ranges and Figure 9 (b) for shorter ranges. The first of these figures, shows various ranges up to 10km using Thorps absorption model (spherical spreading) and has been presented by several authors (Chen & Mitra, 2007; Nasri et al., 2008; Sehgal et al., 2009; Stojanovic, 2006). Figure 9(b) highlights shorter ranges of 500 m and 100 m and also illustrates the variation between the Thorp and Fisher and Simmons absorption loss models developed in Section 3.2.2.

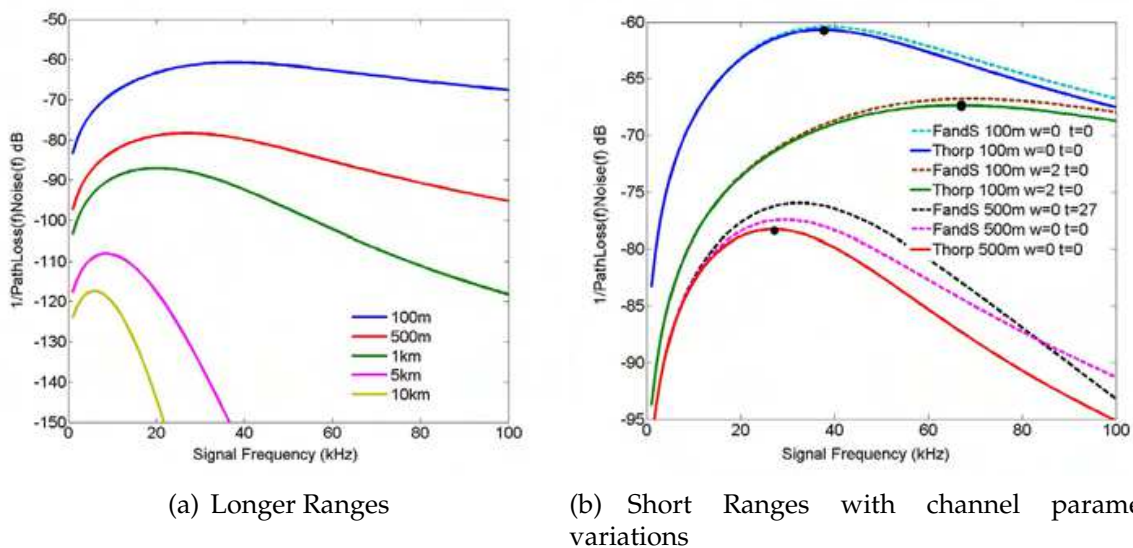
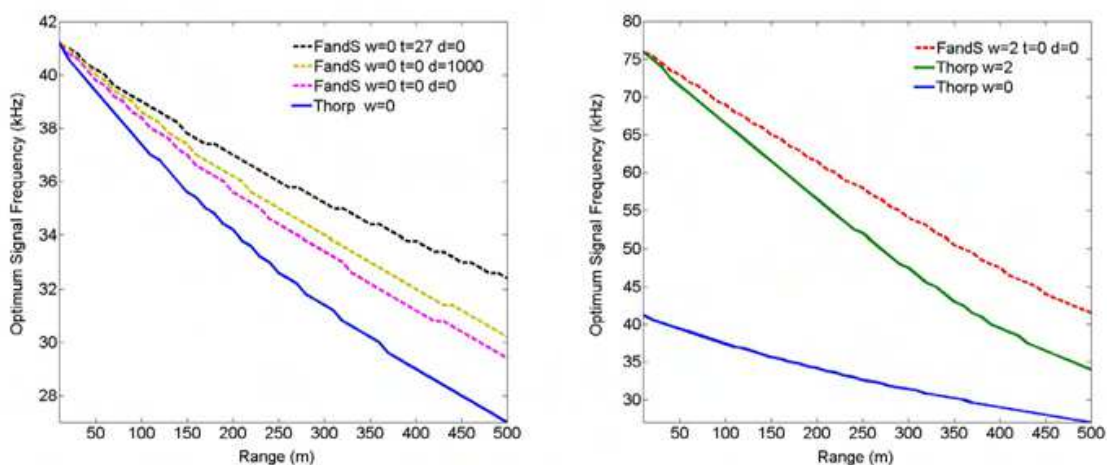


Fig. 9. Frequency Dependent component of narrowband SNR

These figures show that there is a signal frequency where the frequency dependent component of SNR is optimised assuming that the projector parameters, including transmitter power and projector efficiency behave uniformly over the frequency band. The black dot at the apex of each of the three curves based on the Thorp absorption model indicate this optimum point. The two absorption models present similar responses and optimum frequencies. There is a minor variation in optimum frequency at 100 m where the absorption coefficient has a significantly lower contribution. The impact that the Ambient Noise component has on optimum signal frequency is seen most dramatically at the 100 m range when the wind state is changed from 0 to 2 m/s, the optimal signal frequency changes from 38 kHz to 68 kHz. From a communication perspective, if two vehicles were operating at 100 m and 38kHz and the wind state changed from 0 m/s to 2 m/s, there is a reduction of 9dB in the frequency dependent component of SNR. This is not an absolute reduction in SNR as the projector parameters and in particular the transmitter power level has not been considered here. It does however indicate the significant impact that wind and wave action can play with data communication underwater, and in addition this reduced SNR value does not include any increased losses associated with the increase scattering that wave action can generate. The impact of shipping, found in the Ambient Noise term, is not included here as its effect is minor on signal frequencies above 10kHz. In Section 3.2.2 Figure 4, temperature variations were seen to have the most impact on the signal frequency associated with the ranges of interest. Figure 9(b) illustrates this difference in terms of the frequency dependent component of SNR. This is further explored in Figure 10(a) in terms of the signal frequency variations over range.

The impact of changes in range can be seen if the vehicles moved from 100 m to 500 m (at wind state 0 m/s), the optimum signal frequency to maintain highest SNR decreases from 38 kHz to  $\approx 28$  kHz, Figure 9(b). Reduction in signal frequency implies a potential reduction in absolute bandwidth and with that a reduction in data rate which needs to be managed. This will be investigated further in the next sub sections. Figure 10 (a) and (b) show the optimum signal frequency verses range up to 500 m for the various parameters; temperature and depth, within the Thorp and Fisher and Simmons Absorption Loss models as well as the wind in the Ambient Noise model. The optimum frequency, decreases with increasing range due to the dominating characteristic of the absorption loss. It can be seen in Figure 10(a) that as the range increases there is an increasing deviation between the two models and between the parameters within the Fisher and Simmons model. There is approximately a 2.5 kHz difference between the models themselves at 500 m and up to 6 kHz when temperature increases are included. When wind is included, Figure 10(b), there is a dramatic change in optimum signal frequency at very short ranges and this difference reduces substantially over the range shown. This is due to the increasing significance of the Absorption Loss term relative to the constant Ambient Noise term (as it is not range dependent), which reduces the affect of the Noise term and therefore the wind parameter. In both Figure 10(a) and (b), the Fisher and Simmons model provides higher optimum frequencies due to the more accurate inclusion of the relaxation frequencies of boric acid and magnesium sulphate.



(a) Comparison of Absorption Loss Parameters (b) Comparison with changes in wind (from Ambient Noise Characteristics)

Fig. 10. Optimum Frequency determined from frequency dependent component of narrowband SNR

#### 4.2 Channel bandwidth

Having established that at different ranges there is an optimum signal frequency that provides a maximum SNR, assuming constant transmitter power and projector efficiency, there is therefore an associated channel bandwidth with these conditions for different ranges. To determine this bandwidth a heuristic of 3dB around the optimum frequency is used. Following a similar approach to Stojanovic (2006) the bandwidth is calculated according to the frequency range using  $\pm 3$ dB around the optimum signal frequency  $f_o(r)$  which has been chosen as the centre frequency. Therefore, the  $f_{min}(r)$  is the frequency when

$PathLoss(r, d, t, f_o(r))N(f_o(r)) - PathLoss(r, d, t, f)N(f) \geq 3dB$  holds true and similarly for  $f_{max}(r)$  when  $PathLoss(r, d, t, f)N(f) - PathLoss(r, d, t, f_o(r))N(f_o(r)) \geq 3dB$  is true. The system bandwidth  $B(r, d, t)$  is therefore determined by:

$$B(r, d, t) = f_{max}(r) - f_{min}(r) \quad (9)$$

Thus, for a given range, there exists an optimal frequency from which a range dependent 3dB bandwidth can be determined as illustrated in Figure 11. The changes discussed in Section 4.1, related to changes in the optimum signal frequency with changes in range and channel conditions such as temperature, depth and wind. These variations are reflected in a similar manner to the changes seen here in channel bandwidth and in turn will reflect in the potential data transmission rates. Figure 11 demonstrates that both the optimal signal frequency and the 3dB channel bandwidth decrease as range increases. The impact of changing wind conditions on channel bandwidth is significant, however as discussed wind and wave action will also include time variant complexities and losses not included here. Temperature increases show an increase in channel bandwidth, at ranges of interest, due to the reduction in absorption loss as temperature increases, which means some benefits in working in the surface layers. The discussion here highlights that the underwater acoustic channel is severely band-limited and bandwidth efficient modulation will be essential to maximise data throughput and essentially that major benefits can be gained when performing data transmission at shorter ranges or in multi-hop arrangements.

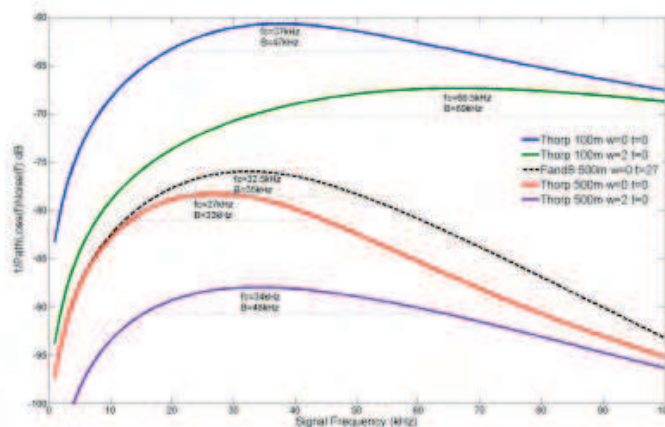


Fig. 11. Range dependent 3dB Channel Bandwidth shown as dashed lines. Where Y-axis is the frequency dependent component of the narrowband SNR

### 4.3 Channel capacity

Prior to evaluating the more realistic performance of the underwater data communication channel, the maximum achievable error-free bit rate  $C$  for various ranges of interest will be determined using the Shannon-Hartley expression, Equation 10. In these channel capacity calculations, all the transmitted power  $P_{tx}$  is assumed to be transferred to the hydrophone except for the losses associated with the deterministic Path Loss Models developed earlier. The Shannon-Hartley expression using the Signal-to-Noise ratio,  $SNR(r)$ , defined in Equation 8, is:

$$C = B \log_2(1 + SNR(r)) \quad (10)$$

where  $C$  is the channel capacity in bps and  $B$  is the channel bandwidth in Hz

Thus using the optimum signal frequency and bandwidths at 100 m and 500 m found in the Section 4.1 and 4.2, the maximum achievable error free channel capacities against range are shown in Figure 12. The signal frequency and channel bandwidth values for 100 m were  $f_o = 37\text{kHz}$  and  $B=47\text{kHz}$  and for 500 m were  $f_o = 27\text{kHz}$  and  $B=33\text{kHz}$ . These are significantly higher than values currently available in underwater operations (Walree, 2007), however they provide an insight into the theoretical limits. Two different transmitter power levels are used, 150dB re  $1\mu\text{Pa}$  which is approximately 10mW (Equation 1) and 140dB re  $1\mu\text{Pa}$  is 1mW. Looking at the values associated with the same power level in Figure 12, the higher channel capacities are those associated with the determined optimum frequency and bandwidth for that range as would be expected. The change in transmitter power, however, by a factor of 10, does not produce a linear change in channel capacity across the range. These variations are important to consider as minimising energy consumption will be critical for AUV operations. In general, current modem specifications indicate possible data rate capacities of less than 10kbps (LinkQuest, 2008) for modem operations under 500 m, well short of these theoretical limits. This illustrates the incredibly severe data communication environment found underwater and that commercial modems are generally not yet designed to be able to adapt to specific channel conditions and varying ranges. The discussion here is to understand the variations associated with the various channel parameters at short range that may support adaptability and improved data transmission capacities.

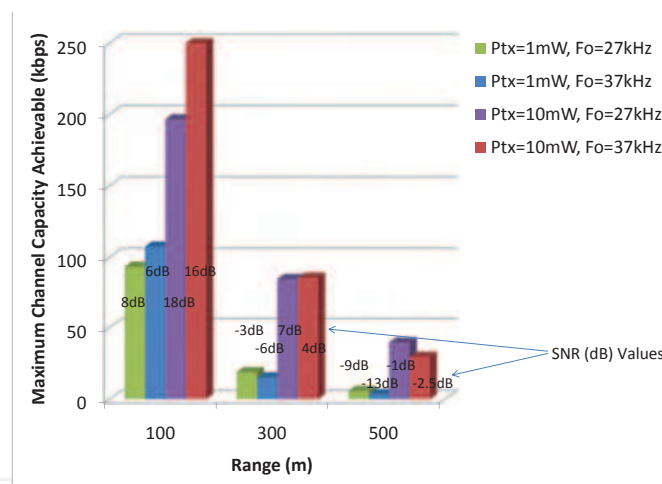


Fig. 12. Theoretical limit of Channel Capacity (kbps) verse Range

#### 4.4 BER in short range underwater acoustic communication

Achieving close to the maximum channel capacities as calculated in the previous section is still a significant challenge in underwater acoustic communication. The underwater acoustic channel presents significant multipaths with rapid time-variations and severe fading that lead to complex dynamics at the hydrophone causing ISI and bit errors. The probability of bit error, BER, therefore provides a measure of the data transmission link performance. In underwater systems, the use of FSK (Frequency Shift Keying) and PSK (Phase Shift Keying) have occupied researchers approaches to symbol modulation for several decades. One approach is using the simpler low rate incoherent modulation frequency hopping FSK

signalling with strong error correction coding that provides some resilience to the rapidly varying multipath. Alternatively, the use of a higher rate coherent method of QPSK signalling that incorporates a Doppler tolerant multi-channel adaptive equalizer has gained in appeal over that time (Johnson et al., 1999).

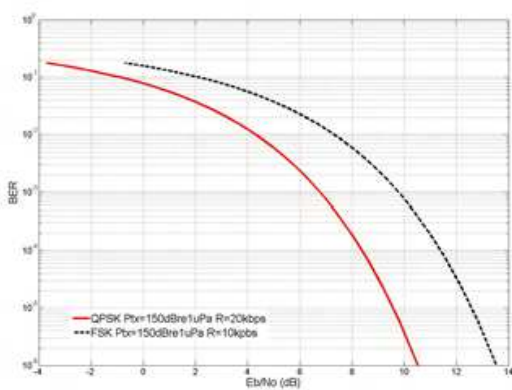
The BER formulae are well known for FSK and QPSK modulation techniques (Rappaport, 1996), which require the Energy per Bit to Noise psd,  $\frac{E_b}{N_o}$ , that can be found from the SNR (Equation 8) by:

$$\frac{E_b}{N_o} = SNR(r) \times \frac{B_c}{R_b} \tag{11}$$

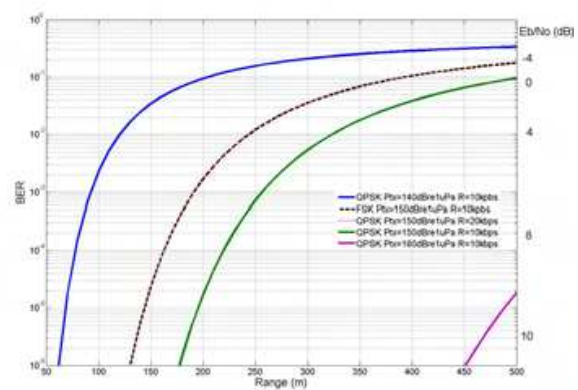
where  $R_b$  is the data rate in bps and  $B_c$  is the channel bandwidth. Equation 12 and 13 are the uncoded BER for BPSK/QPSK and FSK respectively:

$$QPSK : \quad BER = \frac{1}{2} \text{erfc} \left[ \frac{E_b}{N_o} \right]^{1/2} \tag{12}$$

$$FSK : \quad BER = \frac{1}{2} \text{erfc} \left[ \frac{1}{2} \frac{E_b}{N_o} \right]^{1/2} \tag{13}$$



(a) BER vs  $\frac{E_b}{N_o}$



(b) BER vs Range vs  $\frac{E_b}{N_o}$  (for QPSK)

Fig. 13. Probability of Bit Error for Short Range Acoustic Data Transmission Underwater

The data rates  $R_b$  used are 10 and 20 kbps to reflect the current maximum commercial achievable levels. Figure 13 (a) and (b) show the BER for  $\frac{E_b}{N_o}$  and Range respectively. Taking a BER of  $10^{-4}$  or 1 bit error in every 10,000 bits, the  $\frac{E_b}{N_o}$  required for QPSK is 8dB for a transmitter power of 10mW and a data rate of 20kbps. This increases to 12dB if using FSK with half the data rate (10 kbps) and same Transmitter Power. From Figure 13 (b), these settings will provide only a 150 m range. The range can be increased to 250 m using QPSK if the data rate was halved to 10 kbps or out to 500 m if the transmitter power was increased to 100mW in addition to the reduced data rate. Transmitter power plays a critical role, as illustrated here, by the comparison of ranges achieved from  $\approx 75$  m to 500 m with a change of transmitter power needed from 1mW to 100mW for this BER.

## 5. Swarm network protocol design techniques

A short range underwater network, as shown in Figure 1(b) is essentially a multi-node sensor network. To develop a functional sensor network it is necessary to design a number of protocols which includes MAC, DLC (Data Link Control) and routing protocols. A typical protocol stack of a sensor network is presented in Figure 14. The lowest layer is the physical layer which is responsible for implementing all electrical/acoustic signal conditioning techniques such as amplifications, signal detection, modulation and demodulation, signal conversions, etc.. The second layer is the data link layer which accommodates the MAC and DLC protocols. The MAC is an important component of a sensor networks protocol stack, as it allows interference free transmission of information in a shared channel. The DLC protocol includes the ARQ (Automatic Repeat reQuest) and flow control functionalities necessary for error free data transmission in a non zero BER transmission environment. Design of the DLC functionalities are very closely linked to the transmission channel conditions. The network layers main operational control is the routing protocol; responsible for directing packets from the source to the destination over a multi-hop network. Routing protocols keep state information of all links to direct packets through high SNR links in order to minimise the end to end packet delay. The transport layer is responsible for end to end error control procedures which replicates the DLC functions but on an end to end basis rather than hop to hop basis as implemented by the DLL. The transport layer could use standard protocols such as TCP (Transmission Control Protocol) or UDP (User Datagram Protocol). The application layer hosts different operational applications which either transmit or receive data using the lower layers. To develop efficient network architectures, it is necessary to develop network and/or application specific DLL and network layers. The following subsections will present MAC and routing protocol design characteristics required for underwater swarm networking.

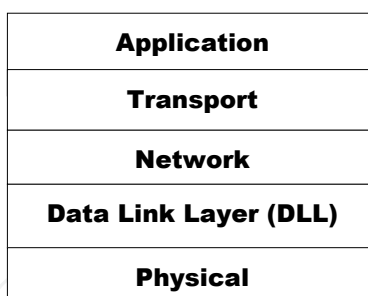


Fig. 14. A typical protocol stack for a sensor network

### 5.1 MAC protocol

Medium access protocols are used to coordinate the transmission of information from multiple transmitters using a shared communication channel. MAC protocols are designed to maximise channel usage by exploiting the key properties of transmission channels. MAC protocols can be designed to allocate transmission resources either in a fixed or in a dynamic manner. Fixed channel allocation techniques such as Frequency Division Multiplexing (FDM) or Time Division Multiplexing (TDM) are commonly used in many communication systems where ample channel capacity is available to transmit information (Karl & Willig, 2006). For low data rate and variable channel conditions, dynamic channel allocation techniques

are generally used to maximise the transmission channel utilisation where the physical transmission channel condition could be highly variable. Based on the dynamic channel allocation technique it is possible to develop two classes of MAC protocols known as random access and scheduled access protocol. The most commonly used random access protocols is the CSMA (Carrier Sense Multiple Access) widely used in many networks including sensor network designs. Most commonly used scheduled access protocol is the polling protocol. Both the CSMA and polling protocols have flexible structures which can be adopted for different application environments. As discussed in this chapter, the underwater communication channel is a relatively difficult transmission medium due to the variability of link quality depending on location and applications. Also, the use of an acoustic signal as a carrier will generate a significant delay which is a major challenge when developing a MAC protocol. In the following subsection we discuss the basic design characteristics of the standard CSMA/CA protocol and its applicability for underwater applications.

### 5.1.1 CSMA/CA protocol

Carrier Sense Multiple Access with Collision Detection protocol is a distributed control protocol which does not require any central coordinator. The principle of this protocol is that a transmitter that wants to initiate a transmission, checks the transmission channel by checking the presence of a carrier signal. If no carrier signal is present which indicates the channel is free and the transmitter can initiate a transmission. For a high propagation delay network such a solution does not offer very high throughput due to the delay.

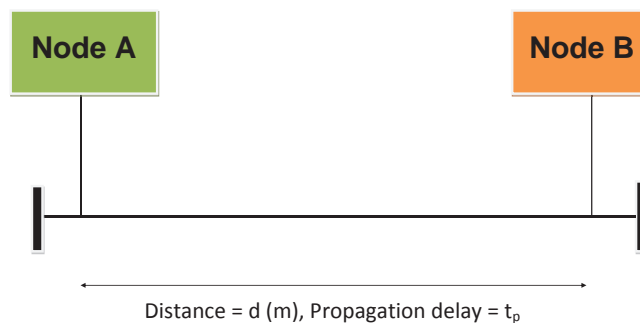


Fig. 15. CSMA/CA protocol based packet transmission example

Consider Figure 15, where two nodes are using CSMA/CA protocol, are spaced apart by 100 meters. In this case, if at  $t=0$ , Node A senses the channel then it will find the channel to be free and can go ahead with the transmission. If Node A starts transmission of a packet immediately then it can assume that the packet will be successfully transmitted. However, if Node B starts sensing the channel before the propagation delay time  $t_p$  then it will also find the channel is free and could start transmission. In this case both packet will collide and the transmission channel capacity will be wasted for a period of  $L+t_p$  where  $L$  is the packet transmission time. On the other hand, if Node B checks the channel after time  $t_p$  from the commencement of A's packet transmission, then it will find the channel is busy and will not transmit any packets. Now this simple example shows how the performance of random access protocol is dependent on the propagation delay. If propagation delay is small then there is much lower probability that a packet will be transmitted before the packet from A arrives at B. As the propagation delay increases the collision probability will also increase.

The CSMA/CA protocol is generally used in RF (Radio Frequency) networks where 100 m link delay will incur a propagation delay of  $0.333 \mu\text{sec}$  whereas an underwater acoustic link

of same distance will generate a propagation delay of 0.29 sec which is about 875,000 times longer than the RF delay. One can easily see why an acoustic link will produce much lower throughput than is predicted by the Shannon-Hartley theorem as discussed in Section 4.3. If we assume that we are transmitting a 100 byte packet, then the packet will take about 0.08 sec to transmit on a 10 kbps RF link. The same packet will take 0.3713 sec on a 10 kbps acoustic link offering a net throughput of 2.154 kbps. This calculation is based on the assumption that the transmission channel is ideal i.e. BER=0. If the BER of the channel is non zero then the throughput will be further reduced.

Previous sections have shown that the BER of a transmission link is dependent on the link parameters, geometry of the application environment, modulation techniques, and presence of various noise sources. Non zero BER conditions introduce a finite packet error rate (PER) on a link which is described by Equation 14, where K represents the packet length. The PER will depend on the BER and the length of the transmitted packet. For a BER of  $10^{-3}$  using a packet size of 100 bytes, the link will generate a PER value of 0.55 which means that almost every second packet will be corrupted and require some sort of error protection scheme to reduce the effective packet error rate.

There are generally two types of packet error correction techniques used in communication systems, one is forward error correction (FEC) scheme which uses a number of redundant bits added with information bits to offer some degree of protection against the channel error. The second technique involves the use of packet retransmission techniques using the DLC function known as the ARQ. The ARQ protocol will introduce retransmissions when a receiver is unable to correct a packet using the FEC bits. The retransmission procedure could effectively reduce the throughput of a link further because the same information is transmitted multiple times. From this brief discussion one can see that standard CSMA/CA protocols used in sensor networks are almost unworkable in the underwater networking environment unless the standard protocol is further enhanced. This is a major research issue which is currently followed up by many researchers and authors. Readers can find some of the current research work on the MAC protocol in the following references (Chirdchoo et al., 2008; Guo et al., 2009; Pompili & Akyildiz, 2009; Syed et al., 2008).

$$\text{PER} = 1 - (1 - \text{BER})^K \quad (14)$$

## 5.2 Packet routing

Packet routing is another challenging task in the underwater networking environment. Packet routing protocols are very important for a multi-hop network because the receivers and the transmitters are distributed in a geographical area where nodes can also change their positions over time. Each node maintains a routing table to forward packets through multi-hop links. Routing tables are created by selecting the best cost paths from transmitters to receivers. The cost of a path can be expressed in terms of delay, packet loss, BER, real monetary cost \$, etc.. For underwater networks, the link delay could be used as a cost metric, to transmit packets with a minimum delay. Routing protocols are generally classified into two classes: distance vector and link state routing protocols (LeonGarcia & Widjaja, 2004). The distance vector algorithms generally select a path from a transmitter to receiver based on shortest path through neighbouring networks. When the status of a link changes, for example, if the delay or SNR of a link is increased then the node next to the link will detect and inform its neighbour about the change and suggest a new link. This process will continue until all the nodes in the network have updated their routing table. The link state routing protocols work



in a different manner. In this case all the link state information is periodically transmitted to all nodes in the network. In case of any change of state of a link, all nodes get notification and modify their routing table. In a swarm network link qualities will be variable which will require regular reconfiguration of routing tables. The performance of routing algorithms is generally determined by a number of factors including the convergence delay. In the case of a swarm network the convergence delay will be a critical factor because of high link delays. For underwater swarm applications, each update within a network will take considerably longer time than a RF network, causing additional packet transmission delays. Hence, it is necessary to develop the network structure in different ways than a conventional sensor network. For example, it may be necessary to develop smaller size clustered networks where cluster heads form a second tier network. Within this topology, local information will flow within the cluster and inter-cluster information will flow through the cluster head network. Cluster based communication architectures are also being used in Zigbee based and wireless personal communication networks (Karl & Willig, 2006). Further research is necessary to develop appropriate routing algorithms to minimise packet transmission delay in swarm networks. Readers can consult the following references to follow some of the recent progress in the area (Aldawibio, 2008; Guangzhong & Zhibin, 2010; LeonGarcia & Widjaja, 2004; Zorzi et al., 2008).

Discussion in this section clearly shows that the MAC and routing protocol designs require transmission channel state information in order to optimise their performance. Due to the high propagation delay of an underwater channel, any change of link quality such as SNR will significantly affect the performance of the network. Hence, it is necessary to develop a new class of protocols which can adapt themselves with the varying channel conditions and offer reasonable high throughput in swarm networks.

## 6. Conclusion

The increasing potential of Autonomous Underwater Vehicle (AUV) swarm operations and the opportunity to use multi-hop networking underwater has led to a growing need to work with a short-range acoustic communication channel. Understanding the channel characteristics for data transmission is essential for the development and evaluation of new MAC and Routing Level protocols that can better utilise the limited resources within this harsh and unpredictable channel.

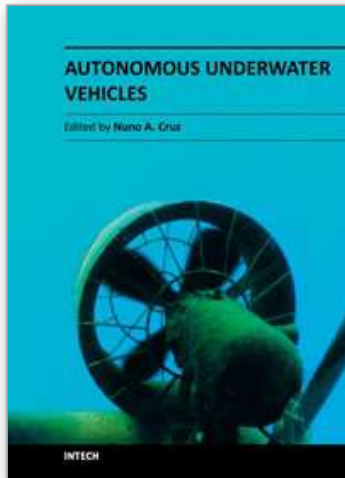
The constraints imposed on the performance of a communication system when using an acoustic channel are the high latency due to the slow speed of the acoustic signal (compared with RF), and the signal fading properties due to absorption and multipath signals, particularly due to reflections off the surface, sea floor and objects in the signal path. The shorter range acoustic channel has been shown here to be able to take advantage of comparatively lower latency and transmitter power as well as higher received SNR and signal frequencies and bandwidths (albeit still only in kHz range). Each of these factors influence the approach needed for developing appropriate protocol designs and error control techniques while maintaining the required network throughput and autonomous operation of each of the nodes in the swarm.

Significant benefits will be seen when AUVs can operate as an intelligent swarm of collaborating nodes and this will only occur when they are able to communicate quickly and clearly between each other in a underwater short range ad-hoc mobile sensor network.

## 7. References

- Aldawibio, O. (2008). A review of current routing protocols for ad hoc underwater acoustic networks, *First International Conference on the Applications of Digital Information and Web Technologies. ICADIWT*, pp. 431–434.
- Caruthers, J. (1977). *Fundamentals of Marine Acoustics*, Elsevier Scientific Publishing.
- Chen, W. & Mitra, U. (2007). Packet scheduling for multihopped underwater acoustic communication networks, *IEEE OCEANS'07*, pp. 1–6.
- Chirdchoo, N., Soh, W. & Chua, K. (2008). Ript: A receiver-initiated reservation-based protocol for underwater acoustic networks, *IEEE Journal on Selected Areas in Communications* 26(9): 1744–1753.
- Coates, R. (1989). *Underwater Acoustic Systems*, John Wiley and Sons.
- Cox, A. W. (1974). *Sonar and Underwater Sound*, Lexington Books.
- Domingo, M. (2008). Overview of channel models for underwater wireless communication networks, *Physical Communication* pp. 163–182.
- Dunbabin, M., Roberts, J., Usher, K., Winstanley, G. & Corke, P. (2005). A hybrid auv design for shallow water reef navigation, *Proc. International Conference on Robotics and Automation (ICRA)*, pp. 2117–2122.
- Eckart, C. (1952). *Principles of Underwater Sound*, Research Analysis Group, National Research Council, California University.
- Essebar, A., Loubet, G. & Vial, F. (1994). Underwater acoustic channel simulations for communication, *IEEE OCEANS '94. 'Oceans Engineering for Today's Technology and Tomorrow's Preservation.'*, Vol. 3, pp. III/495–III/500 vol.3.
- Etter, P. (2003). *Underwater Acoustic Modeling and Simulation*, third edn, Spon Press.
- Fisher, F. & Simmons, V. (1977). Sound absorption in sea water, *Journal of the Acoustical Society of America* 62(3).
- Francois, R. & Garrison, G. (1982). Sound absorption based on ocean measurements: Part 1 and 2, *Journal of the Acoustical Society of America* 72(3,6): 896–907, 1879–1890.
- Guangzhong, L. & Zhibin, L. (2010). Depth-based multi-hop routing protocol for underwater sensor network, *2nd International Conference on Industrial Mechatronics and Automation (ICIMA)*, Vol. 2, pp. 268–270.
- Guo, X., Frater, M. & Ryan, M. (2009). Design of a propagation-delay-tolerant mac protocol for underwater acoustic sensor networks, *IEEE Journal of Oceanic Engineering* 34(2): 170–180.
- Hajenko, T. & Benson, C. (2010). The high frequency underwater acoustic channel, *IEEE OCEANS 2010, Sydney*, pp. 1–3.
- Holmes, J., Carey, W., Lynch, J., Newhall, A. & Kukulya, A. (2005). An autonomous underwater vehicle towed array for ocean acoustic measurements and inversions, *IEEE Oceans 2005 - Europe*, Vol. 2, pp. 1058–1061 Vol. 2.
- Johnson, M., Preisig, J., Freitag, L. & Stojanovic, M. (1999). FSK and PSK performance of the utility acoustic modem, *IEEE OCEANS '99 MTS. Riding the Crest into the 21st Century*, Vol. 3, pp. 1512 Vol. 3.
- Johnson, R. (2011). *University Corporation of Atmospheric Research, Window to the Universe*, University Corporation of Atmospheric Research, <http://www.windows.ucar.edu/tour/link/earth/Water/overview.html>.
- Karl, H. & Willig, A. (2006). *Protocols and Architectures for Wireless Sensor Networks*, John Wiley and Sons, Ltd.

- Kinsler, L., Frey, A., Coppens, A. & Sanders, J. (1982). *Fundamentals of Acoustics*, John Wiley and Sons.
- LeonGarcia, A. & Widjaja, I. (2004). *Communication Networks: Fundamental Concepts and Key Architecture*, second edn, McGraw Hill.
- LinkQuest (2008). *SoundLink Underwater Acoustic Modems, High Speed, Power Efficient, Highly Robust*, LinkQuest Inc., <http://www.link-quest.com/>.
- Mare, J. (2010). Design considerations for wireless underwater communication transceiver, *OCEANS10, Sydney*.
- Nasri, N., Kachouri, A., Andrieux, L. & Samet, M. (2008). Design considerations for wireless underwater communication transceiver, *International Conference on Signals, Circuits and Systems*.
- Parrish, N., Roy, S., Fox, W. & Arabshahi, P. (2007). Rate-range for an fh-fsk acoustic modem, *Proceedings of the second workshop on Underwater networks, WuWNet '07*, pp. 93–96.
- Pompili, D. & Akyildiz, I. (2009). Overview of networking protocols for underwater wireless communications, *IEEE Communications Magazine* 47(1): 97–102.
- Rappaport, T. (1996). *Wireless Communications, Principles and Practice*, Prentice Hall.
- Sehgal, A., Tumar, I. & Schonwalder, J. (2009). Variability of available capacity due to the effects of depth and temperature in the underwater acoustic communication channel, *IEEE OCEANS 2009, EUROPE*, pp. 1–6.
- Stojanovic, M. (2006). On the relationship between capacity and distance in an underwater acoustic communication channel, *International Workshop on Underwater Networks, WUWNet'06*.
- Stojanovic, M. (2008). Underwater acoustic communications: Design considerations on the physical layer, *5th Annual Conference on Wireless on Demand Network Systems and Services, WONS*, pp. 1–10.
- Sullivan, E. & Taroudakis, M. (2008). *Handbook of Signal Processing in Acoustics Volume 2*, RSpringer.
- Syed, A., Ye, W. & Heidemann, J. (2008). Comparison and evaluation of the t-lohi mac for underwater acoustic sensor networks, *IEEE Journal on Selected Areas in Communications* 26(9): 1731–1743.
- Thorp, W. H. (1965). Deep-ocean sound attenuation in the sub- and low-kilocycle-per-second region, *Journal of the Acoustical Society of America* 38(4): 648–654.
- Urick, R. (1967). *Principles of Underwater Sound for Engineers*, McGraw-Hill.
- Waite, A. (2005). *Sonar for Practicing Engineers*, third edn, Wiley.
- Walree, P. (2007). Acoustic modems: Product survey, *Hydro International Magazine* 11(6): 36–39.
- Zorzi, M., Casari, P., Baldo, N. & Harris, A. (2008). Energy-efficient routing schemes for underwater acoustic networks, *IEEE Journal on Selected Areas in Communications* 26(9): 1754–1766.



## **Autonomous Underwater Vehicles**

Edited by Mr. Nuno Cruz

ISBN 978-953-307-432-0

Hard cover, 258 pages

**Publisher** InTech

**Published online** 17, October, 2011

**Published in print edition** October, 2011

Autonomous Underwater Vehicles (AUVs) are remarkable machines that revolutionized the process of gathering ocean data. Their major breakthroughs resulted from successful developments of complementary technologies to overcome the challenges associated with autonomous operation in harsh environments. Most of these advances aimed at reaching new application scenarios and decreasing the cost of ocean data collection, by reducing ship time and automating the process of data gathering with accurate geo location. With the present capabilities, some novel paradigms are already being employed to further exploit the on board intelligence, by making decisions on line based on real time interpretation of sensor data. This book collects a set of self contained chapters covering different aspects of AUV technology and applications in more detail than is commonly found in journal and conference papers. They are divided into three main sections, addressing innovative vehicle design, navigation and control techniques, and mission preparation and analysis. The progress conveyed in these chapters is inspiring, providing glimpses into what might be the future for vehicle technology and applications.

### **How to reference**

In order to correctly reference this scholarly work, feel free to copy and paste the following:

Gunilla Burrowes and Jamil Y. Khan (2011). Short-Range Underwater Acoustic Communication Networks, Autonomous Underwater Vehicles, Mr. Nuno Cruz (Ed.), ISBN: 978-953-307-432-0, InTech, Available from: <http://www.intechopen.com/books/autonomous-underwater-vehicles/short-range-underwater-acoustic-communication-networks>

**INTECH**  
open science | open minds

### **InTech Europe**

University Campus STeP Ri  
Slavka Krautzeka 83/A  
51000 Rijeka, Croatia  
Phone: +385 (51) 770 447  
Fax: +385 (51) 686 166  
[www.intechopen.com](http://www.intechopen.com)

### **InTech China**

Unit 405, Office Block, Hotel Equatorial Shanghai  
No.65, Yan An Road (West), Shanghai, 200040, China  
中国上海市延安西路65号上海国际贵都大饭店办公楼405单元  
Phone: +86-21-62489820  
Fax: +86-21-62489821

© 2011 The Author(s). Licensee IntechOpen. This is an open access article distributed under the terms of the [Creative Commons Attribution 3.0 License](#), which permits unrestricted use, distribution, and reproduction in any medium, provided the original work is properly cited.

IntechOpen

IntechOpen